

Controlled growth of gold nanoparticles on silica nanowires

Aaron D. LaLonde and M. Grant Norton^{a)}

*School of Mechanical and Materials Engineering, Washington State University,
Pullman, Washington 99164-2920*

Daqing Zhang, Devananda Gangadean, Abdullah Alkhateeb, Radhakrishnan Padmanabhan,
and David N. McIlroy

Department of Physics, University of Idaho, Moscow, Idaho 83844-0903

(Received 28 March 2005; accepted 2 August 2005)

Production of gold nanoparticles with the specific goal of particle size control has been investigated by systematic variation of chamber pressure and substrate temperature. Gold nanoparticles have been synthesized on SiO₂ nanowires by plasma-enhanced chemical vapor deposition. Determination of particle size and particle size distribution was done using transmission electron microscopy. Average nanoparticle diameters were between 4 and 12 nm, with particle size increasing as substrate temperature increased from 573 to 873 K. A bimodal size distribution was observed at temperatures ≥ 723 K indicating Ostwald ripening dominated by surface diffusion. The activation energy for surface diffusion of gold on SiO₂ was determined to be 10.4 kJ/mol. Particle sizes were found to go through a maximum with increases in chamber pressure. Competition between diffusion within the vapor and dissociation of the precursor caused the pressure effect.

I. INTRODUCTION

In the United States, the chemical industry produces over 7000 different products worth an estimated \$375 billion per year and generates 10% of the nation's total exports.¹ Eighty percent of processes in the chemical industry use catalysts, and current global catalyst markets are in excess of \$20 billion.² Another major application for catalysts is for carbon monoxide reduction in automobile exhaust systems. The majority of pollution emitted from automobiles is generated in the first 5 min that the engine is running and is a direct result of the inactivity of the current Pt- or Pd-based catalysts below 473 K.³ A possible solution to the limitations presented by existing catalyst materials is the use of Au-based catalysts. In its bulk form Au is very unreactive. However, when the diameter of gold particles is < 10 nm, the activity and selectivity become very structurally sensitive, making Au nanoparticles (NPs) useful in many catalytic reactions.⁴

As a consequence of the increased interest in Au NPs, numerous techniques have been investigated for their production. The most studied techniques are variations

on a general type of precipitation process.⁵⁻⁹ For example, Schimpf et al. used the solution-precipitation approach to coat TiO₂ and ZrO₂ powders with Au NPs.⁹ Particle sizes of approximately 5 nm and 3 nm were obtained for the TiO₂ and ZrO₂ substrates, respectively. Jiang and Gao used carbon nanotubes (CNTs) for the substrate material in a similar process and produced Au NPs with diameters of approximately 10 and 2 nm, depending on whether the substrate surface was acidic or basic.⁶ Using the same type of substrate Han et al.¹⁰ and Wang et al.¹¹ have produced Au NPs using molecularly mediated assembly. Table I summarizes the majority of techniques that have been reported to produce Au NPs.⁵⁻¹⁸ In some of the approaches, Au NPs have been evenly distributed over specific types of nanostructures, while others produced depositions on planar substrates. There is also a large variation in deposition quality among techniques, and only a limited number of systematic studies have been presented to offer a means of tuning the particle size.^{19,20} However, neither of these cited studies examined Au NPs deposited onto substrates.

It has been shown that different substrates are needed for effective catalysis using Au NPs. For example, complete oxidation of CH₄ is most effective when Co₃O₄ is used as the support.⁴ For the decomposition of dioxin, Fe₂O₃ is preferred as the support material.²¹ A technique that is capable of producing NPs on different substrates in a single system setup would be an efficient and economical method for producing catalytic materials.

^{a)}Address all correspondence to this author.

e-mail: norton@mme.wsu.edu
DOI: 10.1557/JMR.2005.0368

TABLE I. Summary of various techniques used to produce Au NPs.

Technique	Au particle size (nm)	Substrate	Reference
Deposition-precipitation	1-7	CNT	5
	10	CNT	6
	1	In Solution	7
	4	In Solution	8
	2-7	ZrO ₂ Particles	9
Molecular assembly	2-5	CNT	10
	12	SiO ₂ /Si Wafer	11
	1-5	Carbon Grid	12
Sonochemical	5	SiO ₂ Microspheres	13
Electroless plating	3-4	CNT	14
Ion implantation	5-10	SiO ₂ /Si Wafer	15
Direct anodic exchange	1-20	Al ₂ O ₃ Powder	16
Aerosol	20	In Gas Phase	17
Chemical vapor deposition	2-7	SiO ₂ Powder	18

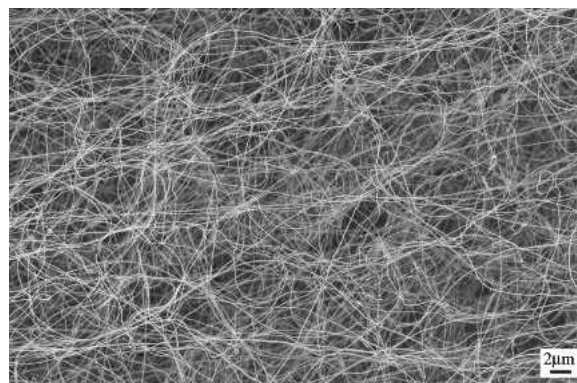
Maximum catalytic activity is also a function of particle size.⁴ For example, the oxidation of CO by Au NPs supported by alkaline earth metal hydroxides requires particles <2 nm in diameter. Photocatalytic hydrogen production using Au NPs supported on TiO₂ is most efficient when particle diameters are approximately 5 nm. Consequently, it becomes very important to be able to predict, control, and produce NPs of a desired size. Tailoring NP size with a selected substrate material will provide maximum efficiency for a catalyst system.

In this paper, we report a systematic study of Au NPs formed on SiO₂ nanowires (NWs) using plasma-enhanced chemical vapor deposition (PECVD). SiO₂ NWs were chosen for this study because of ease of production and availability. They are also very stable at high temperatures, have a high resistance to thermal shock, and provide an inert substrate surface. These characteristics make them ideal for use in applications with varied thermal conditions and where minimal substrate interaction is desired.

II. EXPERIMENTAL DETAILS

The SiO₂ NWs used for this study were produced by a flow furnace technique, similar to that used by Zhang et al.²² They were grown on a Si substrate and have diameters ranging from 30 to 180 nm (Fig. 1). The Au NPs were produced in a custom-designed parallel plate PECVD chamber operated at 13.56 MHz. Argon was used as both the carrier and the background gas. The substrates were mounted on a heated sample holder, which also acted as the grounded anode.

The source compound was 98% pure dimethyl(acetylacetonate)gold (III), obtained from Strem Chemicals Inc. (Newburyport, MA). This material is a white to off-white crystalline solid with a melting temperature of 354 K. It was delivered to the deposition chamber by heating to 303 K in an Ar stream flowing at 10 sccm. The process

FIG. 1. SEM image of SiO₂ NWs used as substrates for Au NPs.

time was 8 min for all samples reported in this study. The total chamber pressure was varied at predetermined settings of 17, 42, and 67 Pa. The substrate temperatures were also varied at fixed values of 573, 723, and 873 K. The effects of different combinations of chamber pressure and substrate temperature on Au NP formation were systematically investigated and are the primary focus of this study.

After deposition the samples were examined using a Philips CM200 (Hillsboro, OR) transmission electron microscope (TEM) and a JEOL 2010 (Peabody, MA) high-resolution TEM (HRTEM), both operated at 200 kV. Sample preparation for TEM characterization consisted of mechanical transference of a small quantity of the NWs from the substrate to a copper grid coated with a lacey carbon support film. Scanning electron microscopy (SEM) images of the original NWs were acquired with a LEO Supra 35 (Thornwood, NY) VP FESEM.

III. RESULTS

Shown in Fig. 1 is a typical SEM image of the SiO₂ NWs that were used as a substrate material for Au NP deposition. The NWs are tens of microns in length and interwoven into a dense mat. For determination of average NP sizes and particle size distributions, several NWs for each deposition condition were analyzed. A minimum of 50 NPs per wire were measured. It was also determined through these measurements that NP diameter appears to be independent of NW diameter.

Bright-field TEM images of Au NPs formed on the NW substrates are shown in Fig. 2. The distinct rings of the inset diffraction pattern in Fig. 2(a) indicate the crystalline nature of the NPs. The SiO₂ NWs are amorphous as evidenced by the absence of clear diffraction maxima. The deposition conditions for the NPs in Fig. 2(a), on a wire 30 nm in diameter, were a substrate temperature of 573 K with a total chamber pressure of 17 Pa. The average NP size for this deposit was determined to be 5 nm, with a standard deviation of 1 nm. The NPs shown in Fig. 2(b) are 7 nm in diameter with a standard deviation

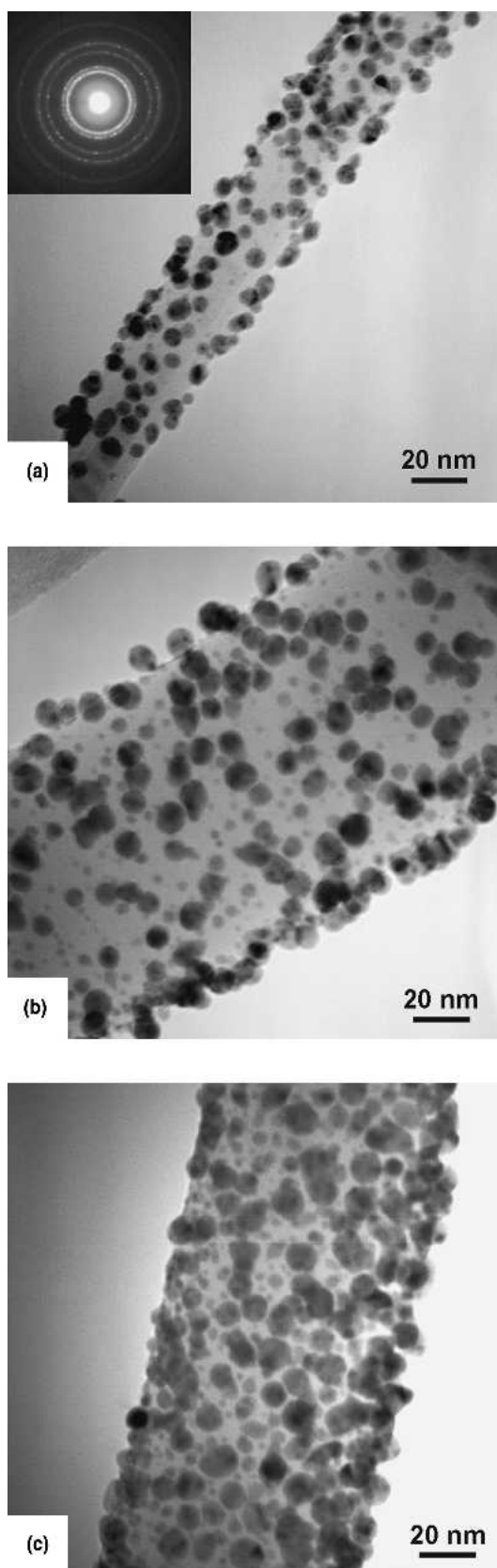


FIG. 2. Bright-field TEM images of Au NPs: (a) on a 30 nm SiO₂ NW, (inset) diffraction pattern; (b) on a 100 nm SiO₂ NW; (c) on a 80 nm SiO₂ NW.

of 2 nm. These NPs were produced at 723 K and 42 Pa on a NW approximately 100 nm in diameter. Figure 2(c) shows a NW of 80 nm in diameter; deposition conditions were 873 K and 17 Pa, resulting in a particle size of 9 nm with a standard deviation of 3 nm. Close inspection of the images in Fig. 2(b) and Fig. 2(c) reveals the presence of two distinct NP sizes on each NW. The smaller particles have an average size of 2 nm in Fig. 2(b) and 3 nm in Fig. 2(c).

The particle size distributions for Au NP deposits at each of 573, 723, and 873 K and a chamber pressure of 67 Pa are shown in Fig. 3. It can be seen from the histograms that a bimodal size distribution was observed only for the Au NPs that were prepared at the two higher temperatures. The size distribution in Fig. 3(a) is Gaussian, with an average particle size of 5 nm. Figure 3(b)

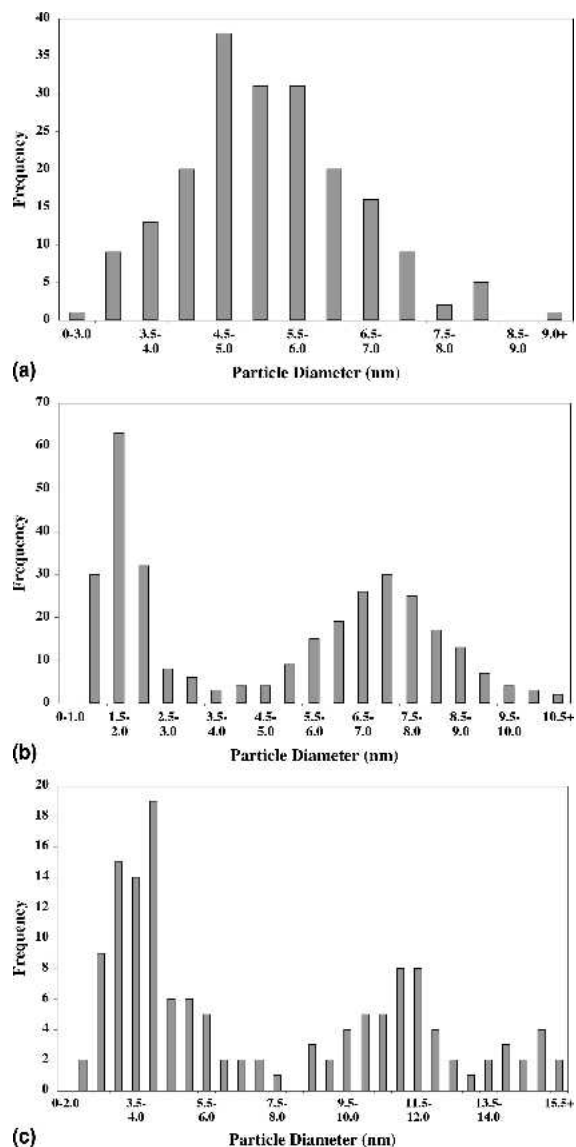


FIG. 3. Histograms showing particle size distributions for Au NPs produced under 67 Pa total chamber pressure: (a) $T = 573$ K, (b) $T = 723$ K, and (c) $T = 873$ K.

shows NPs with average sizes of 7 nm and 2 nm for growth conditions of 723 K and 67 Pa. The particle size distribution for the depositions made at 873 K and 67 Pa are shown in Fig. 3(c), revealing approximate average particle sizes at 12 and 4 nm.

The overall trends of the pressure and temperature effects on particle size were determined and are shown in Fig. 4. In Fig. 4(a) it can be seen that the particle size increases with pressure reaching a maximum at 42 Pa. After this maximum, a continued increase in total chamber pressure causes a decrease in particle size. Also shown in Fig. 4(a) is that as the temperature increases, there is an overall increase in particle size. This trend is clearly evident in Fig. 4(b), which shows that as the substrate temperature increases, there is a corresponding increase in particle size.

Shown in Fig. 5 are HRTEM images of Au NPs deposited on SiO₂ NWs at 723 K and 42 Pa. Figure 5(a) shows a Au NP with a diameter of approximately 8 nm, the inset image is a Au NP 2 nm in diameter from a nearby location. Figure 5(b) shows a faceted Au NP with a diameter of 3 nm. The lattice fringe spacing in this image was measured to be 0.23 nm, corresponding to the {111} planes of Au. The particles shown in Fig. 5(c) have diameters ranging from 5 to 9 nm.

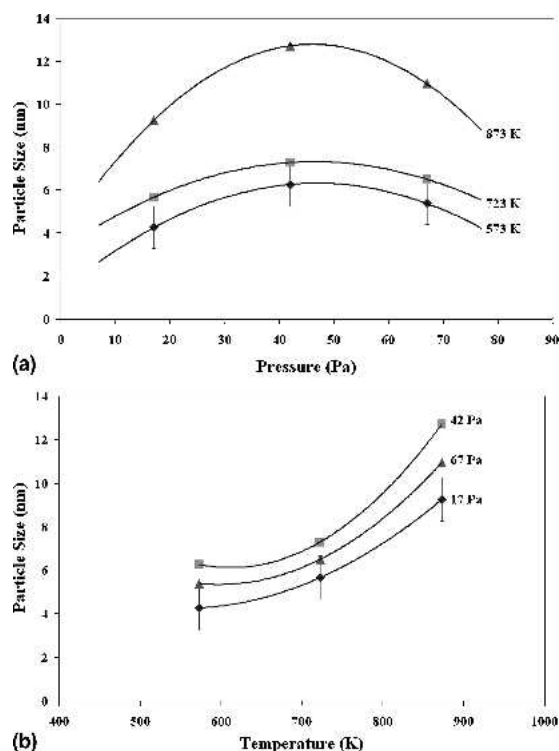


FIG. 4. Pressure and temperature effect on NP size: (a) NP diameter versus pressure and (b) NP diameter versus temperature. The points represent the average particle sizes and similar error bars apply to all data points.

IV. DISCUSSION

Bimodal size distributions of Au NPs have been observed by other groups using different synthesis approaches.^{8,9,12,13,18,20,23,24} Okumura et al.¹⁸ used a chemical vapor deposition (CVD) process with the same precursor as that used in our study and obtained a bimodal size distribution composed of particles approximately 3 and 10 nm in diameter. Pol et al. reported an ultrasound-driven synthesis of Au NPs on silica microspheres in an aqueous solution containing chloroauric acid (HAuCl₄) and ammonia.¹³ When the amount of HAuCl₄ was 0.55 ml per 100 ml of water or greater there was a bimodal size distribution of 2 and 8 nm NPs. Schimpf et al. observed a bimodal size distribution of 2–3 nm and 7–8 nm Au NPs via a deposition-precipitation method also using HAuCl₄ as the precursor.⁹ While these three cited studies reported a bimodal size distribution of Au NPs, no mechanism for this observation was provided.

In contrast, the studies of Kiely et al.,²⁴ Taubert et al.,⁸ and Gutiérrez-Wing et al.¹² have presented possible mechanisms for bimodal size distribution of Au NPs. Kiely et al. reported bimodal size distributions of 5 and 8 nm as well as 5 and 10 nm for Au NPs, prepared by the addition of decanethiol to a toluene solution of colloidal Au. The NPs are thiol-capped, which limits their size during processing. Taubert et al. reported Au NPs precipitated in the presence of a stiff polyphenylene dendrimer template with thiomethyl groups on the outside, resulting in a bimodal size distribution composed of approximately 4 and 20 nm particles. It was suggested, in a manner similar to that of the thiol-capped NPs, that the smaller particles form in the presence of the dendrimer, thus limiting their size to roughly 4 nm, while the larger NPs form from the aggregation of smaller particles. The smaller particles were single crystal, while the larger particles exhibited multiple crystal domains. Gutiérrez-Wing et al. reported synthesis of Au NPs with bimodal size distribution via the Langmuir–Blodgett film growth technique. In this cited study, NPs of approximately 1 and 5 nm were reported, and HRTEM images revealed multiple crystal domains within a single NP, which suggests that the larger particles are the result of the combination of smaller particles.

Based on our observations, the formation of larger particles appears to be a result of the coalescence of smaller particles. Images of NPs 2–3 nm in diameter reveal that they are single crystalline. Larger NPs, possessing diameters of 5–9 nm show several crystalline domains as evidenced by rotationally misoriented lattice planes as well as the presence of moiré fringes in the images. During Ostwald ripening, small particles are consumed by larger particles, the driving force is the reduction of surface free energy, and the result is commonly a bimodal distribution.^{25,26} Mitchell et al. reported

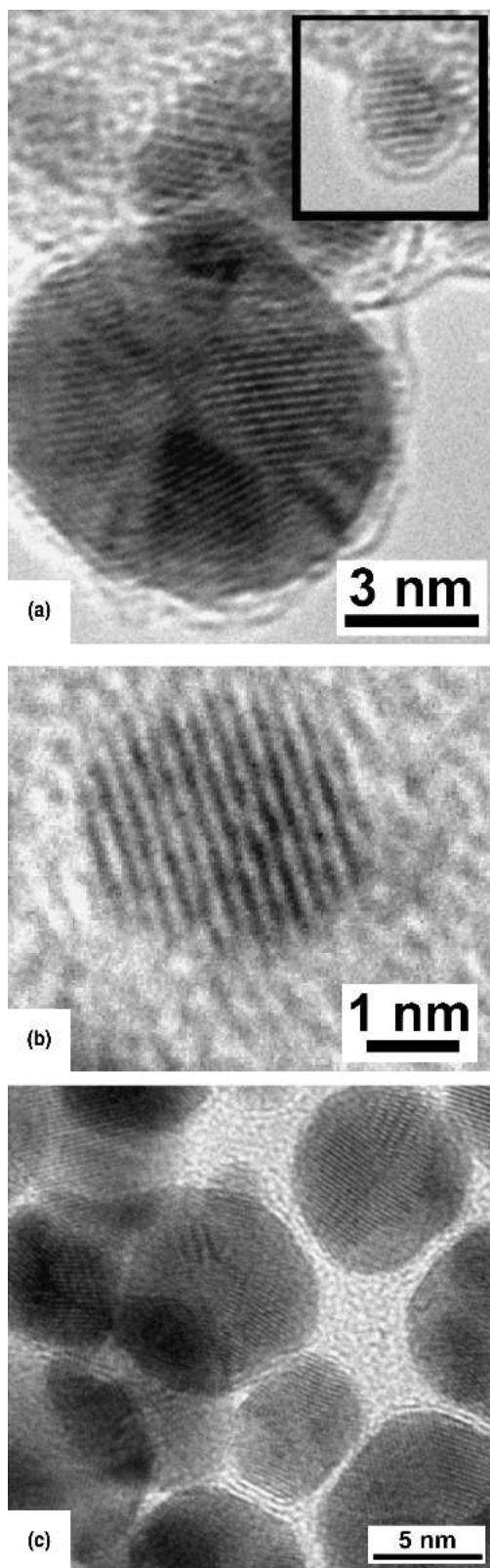


FIG. 5. HRTEM images of Au NPs: (a) 8-nm-diameter particle exhibiting multiple crystal domains, (inset) 2-nm single-crystal particle; (b) 3-nm cuboctahedron with clearly resolved {111} lattice planes; and (c) several NPs ranging in size from 5 to 9 nm showing multiple crystal domains. The background contrast is from the carbon support film.

Ostwald ripening in their study of small gold particles on $\text{TiO}_2(110)$ surfaces.²⁷ There was a narrow size distribution for particles deposited at room temperature, but a bimodal distribution was found after annealing for 7 h at 750 K. These results are consistent with our study. At 573 K, the size distribution is Gaussian, and it is only at temperatures above 723 K that a bimodal distribution was observed. It has been suggested that the low temperatures at which Ostwald ripening occurs for Au NPs may be connected with the depressed melting temperature for small particles.^{28,29}

During CVD processes it is known that there is a direct relationship between temperature and the growth rate of the deposit. This relationship results from surface diffusion effects, which typically follow an Arrhenius behavior

$$D = D_0 \exp \frac{-Q}{RT} \quad (1)$$

D is the diffusion rate, D_0 is a pre-exponential frequency factor, Q is the activation energy, R is the universal gas constant, and T is surface temperature. Surface diffusion is a key component of the process following the adsorption of the precursor material on the substrate. An increase in substrate temperature causes a higher surface diffusion rate, leading to an enhanced growth rate of the deposit. A possible exponential relationship between substrate temperature and particle size is suggested in Fig. 4(b). For each deposition condition, there is an increase in particle size as the temperature of the substrate increases. From these data an activation energy, which will be related to the growth of Au NPs on SiO_2 , was determined by plotting $\ln(\text{particle size})$ versus $1/T$ (the fit for the straight line was $R = 0.9291$). The activation energy was calculated to be 10.4 kJ/mol. This value is within the range of values for heterogeneous surface diffusion of Au. The activation energy for diffusion of Au on $\text{NaCl}(100)$ is ~ 16 kJ/mol and for Au on TiO_2 an energy of 6.6 kJ/mol has been obtained.^{30,31} The implication is that particle growth occurs predominantly by substrate surface diffusion.

The pressure dependence of the particle size is not quite so straightforward, as the change is not monotonic. For all the Au NP deposits that were made, the precursor flow rate was constant. Thus, at any pressure, there exists the same amount of precursor in the vapor phase. As the overall pressure of the chamber increases, there is a decrease in the concentration of the precursor. It would be expected at higher pressures that smaller particle sizes might result. In fact, as shown in Fig. 4(a) the particle size increases as the chamber pressure increases, reaching a maximum, and then the resulting particle size decreases at pressures >42 Pa. This trend may be explained by considering both the effect of the increase in chamber pressure as well as diffusion effects within the vapor.

Under normal CVD conditions, if the flow rate of precursor material is the same at different pressures, there would exist the same amount of material available for deposition. However, in a plasma-enhanced process, the role of pressure is different. In PECVD, the chamber pressure influences the mean free path of the charged species within the plasma, whose purpose is to dissociate the precursor molecules. As the chamber pressure increases, it has been shown that the probability of an ionizing collision in the plasma increases.³² This effect is a direct result of the decreased mean free path in the plasma at higher pressures. It is known from the kinetic theory of gases that the mean free path is inversely dependent on the pressure in the gas. From these considerations, at higher pressures, more of the precursor is dissociated, making more Au available for deposition on the substrate. This in turn leads to an increase in the size of the Au NPs at a given temperature.

The other factor that must be considered is diffusion within the plasma. Again, increasing the chamber pressure will decrease the mean free path of the species in the plasma. As the mean free path decreases, vapor phase diffusion becomes more difficult for all components of the plasma, as shown by Eq. (2)³³

$$D \propto \frac{T^{3/2}}{P}$$

D and T are as defined earlier, and P represents the chamber pressure. It would be expected from the decreased diffusion within the plasma that less Au would reach the surface of the substrate. Therefore, as the diffusion within the plasma decreases, it would be expected that the resultant particle size would decrease. The overall effect of pressure on the size of Au NPs is shown schematically in Fig. 6. The combination of the two individual contributions produces a net effect that qualitatively matches our experimental results.

For NPs a significant fraction of atoms occupy surface sites. Work reported by Schimpf et al.⁹ has suggested that not all the surface sites are equally active for specific reactions. For example, C=O groups are preferentially activated on {111} surfaces and C=C groups may be activated at corner and edge sites. The 3 nm Au NP shown in Fig. 5(b) has the cuboctahedron shape characteristic of many of the smallest particles seen in this study. For such a NP the relative frequency of atoms on corner, (100) face, edge, and (111) face sites is 0.05, 0.10, 0.25 and 0.60, respectively.

Previous research has demonstrated that several methods are capable of producing Au NPs. The most studied of these processes are wet chemical methods, which often involve multiple steps. In these techniques, the preparation of the substrate and solution together with reaction and drying times frequently require several hours each.

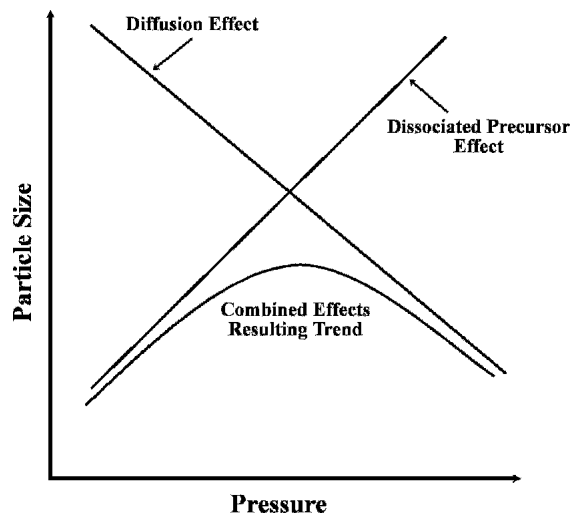


FIG. 6. Schematic showing pressure effects on precursor dissociation and diffusion within the plasma. The combined effects reveal the observed trend for PECVD deposition of Au NPs.

On the other hand, the PECVD method reported here requires significantly less time. Production of the NWs takes on the order of tens of minutes, while the reaction time for the Au NP samples is only 8 min. Using the techniques reported here it is possible to produce NWs, deposit Au NPs of a selected size, and have the sample ready for potential application or characterization in <1 h. The technique is also versatile in that different metal and NW combinations are possible.³⁴

V. CONCLUSIONS

Au NPs were produced on SiO₂ NWs by PECVD. Average particle diameters range from 2 to 12 nm and are a function of the deposition conditions. The diameter of Au NPs was found to increase with pressure, reaching a maximum at 42 Pa and then decreasing. This observation can be explained by considering the competing effects of the pressure dependence of gas-phase kinetics and diffusion rates. The size was also shown to increase exponentially with increases in substrate temperature. At the higher deposition temperatures, there is a bimodal size distribution, which may be explained by Ostwald ripening. The activation energy for particle growth was determined to be 10.4 kJ/mol and indicates a growth process dominated by surface diffusion at constant chamber pressure.

ACKNOWLEDGMENTS

The authors acknowledge the financial support of the W.M. Keck Foundation and the National Science Foundation (Grant Nos. EPS-0132626 and NSF-0138992). The high-resolution TEM work was performed at the Environmental Molecular Science Laboratory, a national

scientific user facility sponsored by the United States Department of Energy's Office (DOE) of Biological and Environmental Research and located at Pacific Northwest National Laboratory, operated for the DOE by Battelle.

REFERENCES

- ATP Focused Program: Catalysis and Biocatalysis Technologies. (2003, April). Retrieved February 12, 2005, from <http://www.atp.nist.gov/atp/focus/cabt.htm>
- Clean Energy and Nano Catalyst Conference, SRI International, Menlo Park, California. (2004, August). Retrieved February 12, 2005, from <http://www.nanoinvestornews.com/>
- C.T. Campbell: The active site in nanoparticle gold catalysis. *Science* **306**, 234 (2004).
- M. Haruta: Size- and support-dependency in the catalysis of gold. *Catal. Today* **36**, 153 (1997).
- B.C. Satishkumar, E.M. Vogl, A. Govindaraj, and C.N.R. Rao: The decoration of carbon nanotubes by metal nanoparticles. *J. Phys. D: Appl. Phys.* **29**, 3173 (1996).
- L. Jiang and L. Gao: Modified carbon nanotubes: An effective way to selective attachment of gold nanoparticles. *Carbon* **41**, 2923 (2003).
- S. Panigrahi, S. Kundu, S.K. Ghosh, S. Nath, and T. Pal: General method of synthesis for metal nanoparticles. *J. Nanoparticle Res.* **6**, 411 (2004).
- A. Taubert, U-M. Wiesler, and K. Müllen: Dendrimer-controlled one-pot synthesis of gold nanoparticles with a bimodal size distribution and their self-assembly in the solid state. *J. Mater. Chem.* **13**, 1090 (2003).
- S. Schimpf, M. Lucas, C. Mohr, U. Rodemerck, A. Brückner, J. Radnik, H. Hofmeister, and P. Claus: Supported gold nanoparticles: In-depth catalyst characterization and application in hydrogenation and oxidation reactions. *Catal. Today* **72**, 63 (2002).
- L. Han, W. Wu, F.L. Kirk, J. Luo, M.M. Maye, N.N. Kariuki, Y. Lin, C-M. Wang, and C-J. Zhong: A direct route toward assembly of nanoparticle-carbon nanotube composite materials. *Langmuir* **20**, 6019 (2004).
- J. Wang, T. Zhu, J. Song, and Z. Liu: Gold nanoparticulate film bound to silicon surface with self-assembled monolayers. *Thin Solid Films* **327-329**, 591 (1998).
- C. Gutiérrez-Wing, J.A. Ascencio, M. Perez-Alvarez, M. Marin-Almazo, and M. Jose-Yacaman: On the structure and formation of self-assembled lattices of gold nanoparticles. *J. Cluster Sci.* **9**, 529 (1998).
- V.G. Pol, A. Gedanken, and J. Calderon-Moreno: Deposition of gold nanoparticles on silica spheres: A sonochemical approach. *Chem. Mater.* **15**, 1111 (2003).
- X. Ma, N. Lun, and S. Wen: Formation of gold nanoparticles supported on carbon nanotubes by using an electroless plating method. *Diamond Relat. Mater.* **14**, 68 (2005).
- L. Guzzi, G. Petö, A. Beck, K. Frey, O. Geszti, G. Molnár, and C. Daróczy: Gold nanoparticles deposited on SiO₂/Si(100): Correlation between size, electron structure, and activity in CO oxidation. *J. Am. Chem. Soc.* **125**, 4332 (2003).
- S. Ivanova, C. Petit, and V. Pitchon: A new preparation method for the formation of gold nanoparticles on an oxide support. *Appl. Catal., A: General* **267**, 191 (2004).
- M.H. Magnusson, K. Deppert, J-O. Malm, J-O. Bovin, and L. Samuelson: Gold nanoparticles: Production, reshaping, and thermal charging. *J. Nanoparticle Res.* **1**, 243 (1999).
- M. Okumura, S. Nakamura, S. Tsubota, T. Nakamura, M. Azuma, and M. Haruta: Chemical vapor deposition of gold on Al₂O₃, SiO₂, and TiO₂ for the oxidation of CO and of H₂. *Catal. Lett.* **51**, 53 (1998).
- M.J. Hostetler, J.E. Wingate, C-J. Zhong, J.E. Harris, R.W. Vachet, M.R. Clark, J.D. Londono, S.J. Green, J.J. Stokes, G.D. Wignall, G.L. Glish, M.D. Porter, N.D. Evans, and R.W. Murray: Alkanethiolate gold cluster molecules with core diameters from 1.5 to 5.2 nm: Core and monolayer properties as a function of core size. *Langmuir* **14**, 17 (1998).
- G. Compagnini, A.A. Scalisi, O. Puglisi, and C. Spinella: Synthesis of gold colloids by laser ablation in thiol-alkane solutions. *J. Mater. Res.* **19**, 2795 (2004).
- M. Haruta: When gold is not noble: Catalysis by nanoparticles. *Chem. Rec.* **3**, 75 (2003).
- H-F. Zhang, C-M. Wang, E.C. Buck, and L-S. Wang: Synthesis, characterization, and manipulation of helical SiO₂ nanosprings. *Nano Lett.* **3**, 577 (2003).
- M.C. Barnes, D-Y. Kim, and N.M. Hwanga: The mechanism of gold deposition by thermal evaporation. *J. Ceram. Proces. Res.* **1**, 45 (2000).
- C.J. Kiely, J. Fink, M. Brust, D. Bethell, and D.J. Schiffrin: Spontaneous ordering of bimodal ensembles of nanoscopic gold clusters. *Nature* **396**, 444 (1998).
- P. Wynblatt and N.A. Gjostein: Particle growth in model supported metal catalysts – I. Theory. *Acta Metal.* **24**, 1165 (1976).
- P. Wynblatt: Particle growth in model supported metal catalysts – II. Comparison of experiment with theory. *Acta Metal.* **24**, 1175 (1976).
- C.E.J. Mitchell, A. Howard, M. Carney, and R.G. Egdell: Direct observation of behaviour of Au nanoclusters on TiO₂(110) at elevated temperatures. *Surf. Sci.* **490**, 196 (2001).
- Ph. Buffat and J-P. Borel: Size effect on the melting temperature of gold particles. *Phys. Rev. A* **13**, 2287 (1976).
- K. Dick, T. Dhanasekaran, Z. Zhang, and D. Meisel: Size-dependent melting of silica-encapsulated gold nanoparticles. *J. Am. Chem. Soc.* **124**, 2312 (2002).
- J.A. Venables: Atomic processes in crystal growth. *Surf. Sci.* **299-300**, 798 (1994).
- S.C. Parker, A.W. Grant, V.A. Bondzie, and C.T. Campbell: Island growth kinetics during the vapor deposition of gold onto TiO₂(110). *Surf. Sci.* **441**, 10 (1999).
- Y.P. Raizer: *Gas Discharge Physics*. (Springer-Verlag, Berlin, Germany, 1991), p. 52.
- M. Ohring: *Materials Science of Thin Films*, 2nd ed. (Academic Press, San Diego, CA, 2002), p. 296.
- A.D. LaLonde, M.G. Norton, D.N. McIlroy, D. Zhang, R. Padmanabhan, A. Alkhateeb, H. Han, N. Lane, and Z. Holman: Metal coatings on SiC nanowires by plasma-enhanced chemical vapor deposition. *J. Mater. Res.* **20**, 549 (2005).